Atmos. Chem. Phys. Discuss., 14, 4303–4325, 2014
www.atmos-chem-phys-discuss.net/14/4303/2014/
doi:10.5194/acpd-14-4303-2014

Atmospheric Chemistry and Physics Discussions

Importance of aerosols for annual lightning production at global scale

S. Venevsky

Center for Earth System Science, Tsinghua University, Haidan, Beijing, 100084, China

Received: 6 December 2013 – Accepted: 28 January 2014 – Published: 17 February 2014

Correspondence to: S. Venevsky (venevsky@mail.tsinghua.edu.cn, sergvene@gmail.com)

Published by Copernicus Publications on behalf of the European Geosciences Union.

Abstract

Lightning production is described using thermodynamic hypotheses mainly according to convective activity in the atmosphere. However, existing formal thermodynamic descriptions are unable to fully explain the profound difference in the flash rate between tropical Africa and South America and between land and ocean. Aerosols are shown to be regulators of lightning in regional studies, but their influence on lightning production at the global scale is not described. I analyzed spatial patterns of the satellite annual global flash rate and simulated, annually averaged cloud condensation nuclei (CCN) distribution and found consistent positive correlation between them for land, ocean and continents. I developed a simple model of lightning production that is based solely on an aerosol hypothesis. The central premise of this model is that concentration of graupel pellets and concentration of ice crystals, which both determine flash rate, are monotonically increasing by CCN concentration up to a critical value (around 2000 cm^{-3}). However, ice crystal concentration falls rapidly after the threshold due to lowering in the number of large cloud droplets effective for rime-splintering ice multiplication. Comparison of the model with a model of the flash rate based on thermodynamic hypotheses demonstrates that the aerosol hypothesis explains the global annual spatial distribution of lightning production consistently better over land and over oceans. My results emphasize importance of aerosols for lightning production and point to the existence of a global aerosol-lightning feedback, which affects both the climate system and the land surface.

1 Introduction

Investigation of the global impact of lightning nitrogen oxide/dioxide on atmospheric ozone and studies of lightning fires require reliable explanation of the global spatial pattern of the flash rate, as seen from global satellite data (e.g. OTD-LIS data (Christian et al., 2003)). Lightning occurs predominantly over land areas in the tropics. Con-

ACPD
14, 4303–4325, 2014

vective climate systems which feature in these regions are associated with a high flash rate (Avila et al., 2010). Explanations of lightning activities are, therefore, initially based on thermodynamic hypotheses. Theoretically derived formal descriptions framed by a thermodynamic hypothesis result in a fifth power relationship between the flash rate and storm height (Williams, 1985) or the difference between the storm height and the cloud freezing level height (Yoshida et al., 2009). Descriptions of global flash rate are also derived from empirical data by fitting polynomials of convective climate variables in accordance with theoretical considerations (Price and Rind, 1992; Allen and Pickering, 2002). However, recent global parameterizations of the flash rate, based on thermodynamic hypotheses, tend to have significant bias in the tropics (Allen and Pickering, 2002) and do not explain the profound difference in the flash rate between the two tropical continental chimneys of Africa and South America (Williams and Satori, 2004) and between land and ocean (Williams and Stanfill, 2002). From regional observation and modeling studies, aerosols are known to be a regulator of cloud microphysics and lightning (Altaratz et al., 2010; Yuan et al., 2011), but their influence on lightning production at global scale has not been described. Simulation of aerosol effects upon electrification and precipitation suggests that charge separation and lightning increases with concentration of cloud condensation nuclei (CCN) up to the threshold of CCN > 2000 cm^{-3} (Mansell and Ziegler, 2013) mainly because of secondary ice multiplication due to rime splintering (the Hallett–Mossop process). Ice multiplication radically reduces after the threshold due to decrease in the number of large droplets and increase in the number of droplets too small to provide effective splintering. In this study I use a correlation analysis and a simple model based on concept of impact of CCN on secondary ice multiplication and lightning production (Mansell and Ziegler, 2013) to analyze how important are aerosols for lightning production at global scale.

ACPD
14, 4303–4325, 2014

2 Positive correlation between flash rate and CCN concentration

To determine if aerosol concentration affects lightning production at global scale, I compared simulated, averaged annual cloud condensation nuclei concentration with the total flash rate (FR) from data observed by satellites (OTD-LIS data) over a 5-year study period (1995–2000). Global annual CCN concentration (see Fig. 1) was calculated as an average of the monthly fields produced in each of 8192 grid cells at the spatial resolution 2.8° by 2.8° longitude/latitude by an emulator (Lee et al., 2013) conditioned on outputs of the state-of-the-art GLOMAP 3-D global aerosol model for the year 2008. Positive correlation was found between global averaged annual CCN concentration and the annually averaged flash rate ($r^2 = 0.53$, $P < 0.001$) which is much stronger than correlation of the total FR with the annually averaged total atmospheric optic depth (AOD) ($r^2 = 0.1$, $P < 0.001$) for the 5-year period (2000–2005). Positive correlation between global averaged annual CCN concentration and the annually averaged flash rate is consistent for pooled land and ocean areas and for individual continents and oceans (see Table 1), ranging from $r^2 = 0.3$ (South America, $P < 0.001$) to $r^2 = 0.74$ (Western part of the Pacific Ocean, $P < 0.001$). The lowest values of r^2 were found in the regions where magnitude of uncertainties in the global model simulation of CCN is the highest both over land (South America) and over ocean (Atlantic Ocean) (Lee et al., 2013).

3 Model of lightning production based on aerosol hypothesis

3.1 Aerosol hypothesis model (AH)

To describe dependence of the annual flash rate by the annually averaged CCN concentration, I used a simple model, which is based solely on the aerosol hypothesis (AH model). Lightning frequency in this model is proportional to the number of collisions between graupel pellets moving downwards and ice crystals moving upwards, similar to other models, which adopt a dipole approach (Baker et al., 1995; Blyth et al., 2001;

ACPD
14, 4303–4325, 2014

Yoshida et al., 2009). Total flash rate is calculated as:

$$f(N_{CCN}) = C \cdot n_{ICE}(N_{CCN}) \cdot n_{GR}(N_{CCN}), \quad (1)$$

where $n_{ICE}(N_{CCN})$ is the concentration of ice particles, $n_{GR}(N_{CCN})$ is the concentration of graupel pellets, N_{CCN} is the CCN concentration and C is a constant. The value of constant C depends on updraft velocity. Updraft velocity is assumed to have low variation with CCN concentration according to 3-D modeling studies (Mansell and Ziegler, 2013) and its influence on flash rate is ignored. Concentration of graupel pellets is monotonically increasing by CCN concentration up to some critical value of N_{CCN}^{crit} (around 2000 cm^{-3} (Mansell and Ziegler, 2013)). Concentration of ice crystals is also increasing simultaneously with concentration of graupel pellets due to secondary ice multiplication with the same speed as $n_{GR}(N_{CCN})$. Flash rate is represented by a power function:

$$f(N_{CCN}) = A \cdot (N_{CCN})^{2\alpha} \quad (2)$$

up to the threshold N_{CCN}^{crit}, where α is between 0.5 and 1 (Mansell and Ziegler, 2013). Concentration of graupel pellets is assumed to continue to monotonically increase with the CCN concentration in charge separation zone of a cloud after the threshold, but the ice crystal concentration is falling rapidly due to lowering in a number of large cloud droplets (more than 24 µm diameter), which are effective for rime-splintering Hallet–Mossop ice multiplication (Mansell and Ziegler, 2013). I adopt the same exponential decay for number of ice particles produced in the Hallet–Mossop process, as decay in number of large cloud drops, effective in splintering, similarly to simplest case in (Ziegler et al., 1986):

$$n_{ICE}(N_{CCN}) \propto (N_{CCN})^{\alpha} e^{\left(-\gamma \frac{V^*}{V}\right)}, \quad (3)$$

where V^* is the 24 µm diameter sphere volume, V is the mean drop volume, γ is a constant. Number of small non-effective in ice multiplication drops is set to be linearly

ACPD
14, 4303–4325, 2014

dependent from CCN concentration exceeding critical, so as the proportion of volumes

$$\frac{V^*}{V}(N_{CCN}) = \theta \cdot (N_{CCN} - N_{CCN}^{crit}), \quad (4)$$

where θ is a constant. Loss of the number of collisions after the threshold N_{CCN}^{crit} is translated into the flash rate:

$$f(N_{CCN}) = A \cdot (N_{CCN})^{2\alpha} \cdot e^{\left(-\lambda\left(N_{CCN} - N_{CCN}^{crit}\right)\right)}, \quad (5)$$

where λ is a constant.

3.2 Fitting of the aerosol hypothesis model

This aerosol based model was fit to the observed OTD-LIS annual flash rate with the simulated annually averaged CNN concentration (see Fig. 2) using logarithmic regression. The critical value of CCN concentration ($2380\,cm^{-1}$), where lightning production starts to decrease N_{CCN}^{crit} was taken from a grid cell where the annual flash rate had its maximum ($71\,fl\,yr^{-1}\,km^{-2}$). The value of N_{CCN}^{crit} coincides with a value of AOD = 0.263 if we calculate annually averaged AOD for the years 2000–2005 from the linear regression on the simulated annually averaged CNN concentration ($r^2 = 0.24$, $p < 0.001$). This is a close match to the AOD value of 0.25, where lightning production was observed to start a decline described by (Altaratz et al., 2010) and (Yuan et al., 2012) In order to find three other parameters of AH model (A, α, λ) all observed OTD-LIS gridded flash rate data set $LF^{OTD}(longitude, lattitude)$ was partitioned as follows: the first subset where the grid cells had value of CCN concentration less or equal than the critical value $N_{CCN}^{\leq} N_{CCN}^{crit}$ and the second subset where these values were greater than the critical one $N_{CCN}^{>} N_{CCN}^{crit}$.

ACPD
14, 4303–4325, 2014

Linear regression for logarithms of the annual flash rate LF_{reg}^{OTD} on the averaged annually CCN concentration N_{CCN} was calculated for the first subset ($r^2 = 0.58$, $p < 0.001$):

$$\ln(LF_{reg}^{OTD}) = a \cdot \ln(N_{CCN}) + b, \quad (6)$$

where $a = 1.67$, $b = -10.43$.

Ratio of observed annual OTD-LIS flash rate to the annual flash rate calculated from the regression Eq. (6) $\frac{LF^{OTD}}{LF_{reg}^{OTD}} = \frac{LF^{OTD}}{e^{b} \cdot (N_{CCN})^{a}}$ was used to estimate the exponent of decline in lightning production λ at the second subset of observed OTD-LIS flash rate gridded data.

Linear regression was calculated ($r^2 = 0.32$, $p < 0.001$) for the logarithm of this ratio by the excess in CCN concentration to critical value 2381 cm^{-3} $N_{CCN}^{Excess} = N_{CCN} - 2381$ (see Fig. 3 for the logarithm of the ratio by the excess CCN concentration function):

$$\ln\left(\frac{LF^{OTD}}{LF_{reg}^{OTD}}\right) = -\lambda N_{CCN}^{Excess} + I, \quad (7)$$

where $\lambda = 0.0007$, $I = 0.32$.

Final parameters of the model AH (equations 2 and 6) based on the atmospheric hypothesis are $A = e^{b} \cdot 1.62 = 0.000048$ fl yr^{-1} km^{-2}, $\alpha = a/2 = 0.835$, $\lambda = 0.0007$ and $N_{CCN}^{crit} = 2381$ cm^{-3} (coefficient A was inflated for a better fit).

Annual flash rate in the suggested formulation drops with the annually averaged CCN concentration to 0.6 flashes per year in a square kilometer at $N_{CCN} = 8000$ cm^{-3} and vanishes almost completely after $N_{CCN} > 10\,000$ cm^{-3} (see Fig. 2)

ACPD
14, 4303–4325, 2014

4 Model of lightning production based on thermodynamic hypothesis

4.1 Thermodynamic hypothesis model (TH)

The parameterizations of lightning flash rate in terms of convective precipitation for land and ocean (Allen and Pickering, 2002) were taken from the model which is solely based on the thermodynamic hypothesis:

$$\mathrm{LF_{CG}}(P) = A_i \cdot (a + bP + cP^2 + dP^3 + eP^4)/A, \quad (8)$$

where $\mathrm{LF_{CG}}$ is the cloud-to-ground flash rate (flashes min^{-1}), A_i is the area of the grid box, A is the area of a $2.0^\circ \times 2.5^\circ$ box centered at 30° N, P is the convective precipitation ($\mathrm{mm\,day}^{-1}$) and a–e are coefficients (land $a = 3.75 \times 10^{-2}$, $b = -4.76 \times 10^{-2}$, $c = 5.41 \times 10^{-3}$, $d = 3.21 \times 10^{-4}$, $e = -2.93 \times 10^{-6}$ and ocean $a = 5.23 \times 10^{-2}$, $b = -4.80 \times 10^{-2}$, $c = 5.45 \times 10^{-3}$, $d = 3.68 \times 10^{-5}$, $e = -2.42 \times 10^{-7}$).

This parameterization was designed using data for flash rates over the United States in 1997 from the US National Lightning Detection Network (NLDN) and the US Long Range Flash Network (LFR). Convective fields from the Goddard Earth Observing System Data Assimilation System (GEOS DAS) were used in the design of a polynomial regression for the flash rate. The parameterization was compared by (Allen and Pickering, 2002) with other mathematical formulations of the flash rate using convective mass flux (for cloud-to-ground flashes) and cloud top height (inter-cloud and cloud-to-ground flashes). Thermodynamic formulations by convective precipitation and convective mass flux were recalculated to the total (inter-cloud and cloud-to-ground) lightning production LF by multiplying $\mathrm{LF_{CG}}$ by the empirical function of latitude L (Price and Rind, 1993), also adopted in this study. The total flash rate LF was estimated from the cloud-to-ground (CG) flash rate $\mathrm{LF_{CG}}$ as:

$$\mathrm{LF} = \mathrm{LF_{CG}}/f_{\mathrm{CG}}(\Delta z), \quad (9)$$

where $f_{\mathrm{CG}}(\Delta z)$ is the fraction of CG flashes, which can be calculated as a fourth power polynomial of the depth Δz of the cloud above freezing level (Price and Rind, 1993).

ACPD
14, 4303–4325, 2014

The fraction of CG flashes $f_{CG}(\Delta z)$ varies between 0.25 at the equator to 0.35 at high latitudes and can be calculated approximately as a function of latitude L (Price and Rind, 1993):

$$f_{CG}(\Delta z) = a + b\Delta z + c\Delta z^2 + d\Delta z^3 + e\Delta z^4, \quad (10)$$

where $a = 63.09$, $b = -36.54$, $c = 7.439$, $d = -0.648$, $e = 0.021$, $\Delta z = mL^2 + nL + o$ and $m = -0.0000664$, $n = -0.00473$, $o = 7.34$.

Finally all three climatic parameterizations were checked against the Optical Transient Detector total flash rate data for different seasons, oceanic or land locations. Because the ratio of the number of global 1996 flashes over and near land in 1996 to that over marine locations calculated from convective precipitation was closest to the ratio observed by OTD (see Table 2 and 3 of (Allen and Pickering, 2002)), I chose a convective precipitation based thermodynamic model for this study.

Daily NCEP convective precipitation data (http://www.esrl.noaa.gov/psd/) for the period 1995–2000 were linearly interpolated from the T62 Gaussian grid to 2.8125° × 2.8125° longitude/latitude resolution and used for the calculation of the daily total flash rate LF(P) from an initial parameterization (Allen and Pickering, 2002) separately for land and ocean at global scale. The calculated, spatially distributed daily flash rate was summed over each year and averaged over the five-year period.

4.2 Correction of the thermodynamic hypothesis model

Additional fitting of the TH model was done to provide fair comparison with the AH model.

To make the initial parameterization (see Eqs. 8–10) closer to the OTD average annual flash rate LF^{OTD} data for the period 1995–2000. I performed a simple polynomial transformation of LF at global scale separately for land and ocean. This transformation was based on a logarithmic regression of the annually averaged observed OTD annual flash rate LF^{OTD} on annual flash rate from the parameterization by convective precipi-

ACPD
14, 4303–4325, 2014

tation LF(P). The best fits for land and ocean were provided by following functions:

$$\begin{aligned} \mathrm{LF}^{\mathrm{fit}}(P) &= K \cdot (\mathrm{LF}(P))^{\beta} + L, \qquad \text{for land} \\ \mathrm{LF}^{\mathrm{fit}}(P) &= M \cdot (\mathrm{LF}(P))^{\gamma} + R, \qquad \text{for ocean} \end{aligned} \tag{11}$$

where for land $K = 1$, $\beta = 1.02$, $L = 1.95$ and for ocean $M = 0.25$, $\gamma = 1.2$ and $R = 0.02$.

The fitting of the flash rate results in a small increase in correlation coefficient between OTD and the theoretical thermodynamic model for land and ocean. It can be seen that an initial parameterization (Allen and Pickering, 2002) for land experiences very little change after the transformation (both power coefficient β and slope coefficient K stay close to 1). Thus, description of the flash rate by convective precipitation at land cannot be further improved without considering additional factors. Power coefficient γ and slope coefficient M in the new parameterization are both different from 1 for the ocean. This fact points to a moderate ability of convective precipitation as a basic climate variable for description of lightning over the ocean at global scale.

I consider the new transformed parameterization to be the basic model of annual flash rate based on a thermodynamic hypothesis (TH model) for further inter-model comparison exercise:

$$f(P) = \mathrm{LF}^{\mathrm{fit}}(P) \tag{12}$$

5 Comparison of models based on aerosol and thermodynamic hypotheses

The global model of lightning production based solely on the aerosol hypothesis has a strong positive correlation with the observed annual flash rate data for the globe ($r^2 = 0.59$, $p < 0.001$), the entire land ($r^2 = 0.49$, $p < 0.001$) and the entire ocean ($r^2 = 0.37$, $p < 0.001$). Slope of the regression between observed and simulated flash rates is approximately 1.0 for the globe, 1.01 for the land and 0.65 for the ocean.

Comparison between the models based on two different hypotheses (see Fig. 4) reveals that they both can reproduce global observed mean and standard deviation

ACPD
14, 4303–4325, 2014

of the annual flash rate (see Table 2). However, the TH model cannot correctly represent the overall spatial distribution of annual flash rate in the tropical belt (30° N–30° S), placing areas in Africa far from the observed average mean and standard deviation (see Table 2). The AH model predicts the mean and standard deviation for Africa more accurately (see Table 2), both in absolute values and relative to the predictions for the Americas and Maritime Continents (Asia and Australia). The solely aerosol based annual flash rate model outperforms the thermodynamic one at all continents and oceans (see Table 3), resulting in better correlations (presented as multiple R for observed/simulated linear regression) and better fit (presented as a value of slope of the observed/simulated linear regression). The model based on aerosol hypothesis demonstrates the best result over West part of the Pacific Ocean, where an evidence of aerosol enhancement of lightning activity was observed at inter-annual and bi-weekly time steps (Yuan et al., 2011). Here CCN concentration is at its lowest which makes annual flash in the area most sensitive to non-homogeneities in aerosol distribution. The AH model does not distinguish maximums in lightning production between continents in the tropics due to its statistical design, while the TH model incorrectly estimates continental maxima (see Table 2).

6 Conclusions

Thus, the annually averaged CCN concentration is an important driving force in the spatial distribution of the annual flash rate at global scale. An increase in CCN concentration plays a dual role in determining of the flash rate value. First, the increase of CCN concentration influences growth in lightning production due to general growth in mass of electrifying hydrometeors (graupel and ice crystals from secondary ice multiplication). Further increase, after crossing the critical value of CCN concentration, affects lightning production negatively, because at high aerosol concentrations, a drop in ice crystal mass relates to low availability of large cloud drops effective in rime-splintering ice multiplication.

ACPD
14, 4303–4325, 2014

Large scatter of the observed annual flash rate by the simulated CCN concentration around the AH model output (see Fig. 1) demonstrates that local thermodynamic conditions should be included in this model for better predictions at the annual time step. Graupel mass can become steady or slightly decrease after the critical threshold in CCN concentration (Mansell and Ziegler, 2013) in certain meteorological conditions, pushing lightning production down. Local cloud base height or updraft velocity variation may change vertical entrainment of aerosols and alter the vertical distribution of electrifying hydrometeors, affecting local flash rate.

As for the finer than annual time steps, many studies showed that lightning production, described by related indices (Schummann resonances or other) is positively correlated to surface temperature at diurnal and daily time scale for tropical regions (Price, 2013). These findings demonstrated that description of atmospheric thermodynamic instability is most likely necessary for estimating of the flash rate at diurnal, monthly and possibly seasonal time steps.

The results of this study point to the existence in the Earth system of a global aerosol-lightning feedback that impacts both the climate system and the land surface. Anthropogenic emissions have increased the mean global CCN concentration in the lower troposphere by 60–80 % since the preindustrial period (Yu et al., 2013). According to the presented AH model, the growth in CCN concentration could have increased lightning production since preindustrial times in a majority of regions outside the tropics and decreased it in regions of extreme air pollution such as North East China,. This trend of global lightning increase (except South East Asia) will likely to continue, but may be slowed by implementation of air quality regulations in emerging economies. Climate change can cause inter-annual redistribution of the daily flash rate as a result of both increase in daily surface temperatures and variation in daily CCN concentration driven by atmospheric circulation and aerosol emissions. Potential future growth in lightning production associated with potential anthropogenic CCN increase and global warming may result in positive feedback due to release of nitrogen oxides (NO_x) and increase in photolysis reaction of tropospheric ozone (O_3), a strong greenhouse gas.

ACPD
14, 4303–4325, 2014

Despite increase in amount of greenhouse gas ozone, on the same time realized OH reduces the lifetime of methane, also a greenhouse gas (Schumann and Huntrieser, 2007). The modeling studies with a 10 % lightning NOx increase (0.5 $Tg\,N\,yr^{-1}$) show an integrated cooling (negative radiative forcing 2 $mW\,m^{-2}\,yr^{-1}$) as a result of interplay between negative perturbation of methane and positive perturbation of ozone (Wild et al., 2001). Although lightning NOx, O_3 and reduced CH_4 have a small contribution to overall radiative forcing, their impacts upon the upper troposphere in the tropics may be significant (Price, 2013).

Another positive feedback potentially amplifying global warming with atmospheric CCN concentration growth is associated with lightning fires, which claim thousands of square kilometers of forests in boreal, temperate and Mediterranean zones each year. Wildfires release considerable amounts of aerosols and greenhouse gas species (Clinton et al., 2006), affecting the climate system regionally and globally. The aerosols released from biomass burning may affect lightning frequency positively or negatively according to observations (Altaratz et al., 2010) and the AH model, accelerating or slowing onset of wildfires.

Appendix A

Data source

Total (inter-cloud and cloud-to-ground) lightning production, expressed as a flash rate density (fl/km2/yr) were downloaded from ftp://ghrc.nsstc.nasa.gov/pub/lis/climatology/HRFC/data/. This is a 0.5° × 0.5° gridded product containing climatologies from the 5 yr OTD (April 1995–March 2000) and 5 yr LIS (December 1997–December 2000), which was further aggregated to 2.8125° × 2.8125° (resolution of climate data).

Global averaged annual cloud condensation nuclei concentration was calculated as average of the monthly fields of CCN concentration at an altitude of 915 hPa at 2.8125° × 2.8125° longitude/latitude resolution for a one representative year (2008).

ACPD
14, 4303–4325, 2014

The fields include mean values across all important 28 parameter uncertainty spaces of the GLOMAP 3-D aerosol model (Lee et al., 2013).

Annual averaged aerosol optical depth for the period 2001–2005 at 2.8125°×2.8125° longitude/latitude resolution was retrieved using the NASA GIOVANNI system (http://gdata1.sci.gsfc.nasa.gov/daac-bin/G3/gui.cgi?instance_id=aerosol_daily).

Daily NCEP data NCEP convective precipitation Reanalysis data for the period 1995–2000 was provided by the NOAA/OAR/ESRL PSD, Boulder, Colorado, USA, from their Web site at http://www.esrl.noaa.gov/psd/.

References

Allen, D. J. and Pickering, K. E.: Evaluation of lightning flash rate parametrisations for use in a global chemical transport model, J. Geophys. Res., 107, 4711, doi:10.1029/2002JD002066, 2002.

Altaratz, O., Koren, I., Yair, Y., and Price, C.: Lightning response to smoke from Amazon fires, Geophys. Res. Let., 37, L07801, doi:10.1029/2010GL042679, 2010.

Avila, E. E., Burgesser, R. E., Castellano, N. E., Collier, A. B., Compagnucci, R. H., and Hughes, A. R. W.: Correlations between deep convection and lightning activity on a global scale, J. Atmos. Sol.-Terr. Phy., 72, 1114–1121, 2010.

Baker, M. B., Christian, H. J., and Latham, J.: A computational study of the relationship linking lightning frequency and other thundercloud parameters, Q. J. Roy. Meteor. Soc., 121, 1525–1548, 1995.

Blyth, A. M., Christian, H. J., Driscoll, K. T., Gadian, A. M., and Latham, J.: Determination of ice precipitation rates and thunderstorm anvil ice contents from satellite observation of lightning, Atmos. Res., 59–60, 217–229, 2001.

Christian, H. J., Blakeslee, R. J., Boccippio, D. J., Buechler, D. E., Driscoll, K. T., Goodman, S. J., Hall, J. M., Koshak, W. J., Mach, D. M., and Stewart, M. F.: Global frequency of lightning as observed from space by the Optical Transient Detector, J. Geophys. Res., 108, 4005, doi:10.1029/2002JD002347, 2003.

Clinton, N. E., Gong, P., and Klaus, S.: Quantification of pollutants emitted from very large wildland fires in Southern California, USA, Atmos. Environ., 40, 3686–3695, 2006.

ACPD
14, 4303–4325, 2014

Warwick, N. J., Archibald, A. T., Ashworth, K., Dorsey, J., Edwards, P. M., Heard, D. E., Langford, B., Lee, J., Misztal, P. K., Whalley, L. K., and Pyle, J. A.: A global model study of the impact of land-use change in Borneo on atmospheric composition, Atmos. Chem. Phys., 13, 9183–9194, doi:10.5194/acp-13-9183-2013, 2013.

Mansell, E. and Ziegler, C. L.: Aerosol effects on simulated storm electrification and precipitation in a two-moment bulk microphysics model, J. Atmos. Sci., 70, 2032–2050, 2013.

Price, C. and Rind, D.: A simple lightning parametrisation for calculating global lightning activity, J. Geophys. Res., 97, 9919–9993, 1992.

Price, C. and Rind, D.: What determines the cloud-to-ground lightning fraction in the thunderstorms?, Geophys. Res. Lett., 20, 1993, 1993.

Price, C.: Lightning applications in weather and Clim. Res., Surv. Geophys., 34, 755–767, 2013.

Schumann, U. and Huntrieser, H.: The global lightning-induced nitrogen oxides source, Atmos. Chem. Phys., 7, 3823–3907, doi:10.5194/acp-7-3823-2007, 2007.

Wild, O., Prather, M. J., and Akimoto, H.: Indirect long-term cooling from NO_x emissions, Geophys. Res. Lett., 28, 1719–1722, 2001.

Williams, E.: Large scale charge separation in thunderclouds, J. of Geophys. Res., 90, 6013–6025, 1985.

Williams, E. and Stanfill, C. R.: The physical origin of the land–ocean contrast in lightning activity, C. R. Phys., 3, 1277–1292, 2002.

Williams, E. and Satori, G.: Lightning, thermodynamics and hydrological comparison of the two tropical continental chimneys, J. Atmos. Sol.-Terr. Phy., 66, 1213–1231, 2004.

Yoshida, S., Morimoto, T., Ushio, T., and Kawasaki, Z.: A fifth-power relationship for lightning activity from Tropical Rainfall Measuring Mission satellite observations, J. Geophys. Res., 114, D09104, doi:10.1029/2008JD010370, 2009.

Yu, F., Ma, X., and Luo, G.: Anthropogenic contribution to cloud condensation nuclei and the first aerosol indirect climate effect, Environ. Res. Lett., 8, 024029, doi:10.1088/1748-9326/8/2/024029, 2013.

Yuan, T., Remer, L. A., Pickering, K. E., and Yu, H.: Observational evidence of aerosol enhancement of lightning activity and convective invigoration, Geophys. Res. Lett., 38, L04701, doi:10.1029/2010GL046052, 2011.

ACPD
14, 4303–4325, 2014

Yuan, T., Remer, L. A., Bian, H., Ziemke, J. A., Albrecht, R., Pickering, K. E., Oreopoulos, R., Goodman, S. J., Yu, H., and Allen, D. J.: Aerosol indirect effect on tropospheric ozone via lightning, J. Geophys. Res., 117, D18213, doi:10.1029/2012JD01772, 2012.

Ziegler, C. L., Ray, P. S., and MacGorman, D. R.: Relations of kinematics, microphysics and electrification in an isolated mountain thunderstorm, J. Atmos. Sci., 43, 2098–2113, 1986.

ACPD

14, 4303–4325, 2014

Table 1. Correlation between global averaged annual CCN concentration and the annually averaged flash rate.

Region	r^2	p value	F
Globe	0.54	0	9669.676
Land	0.43	1.2×10^{245}	1506.583
Ocean	0.4	0	3749.316
North America	0.5	1.34×10^{-67}	434.6495
South America	0.3	9.37×10^{-17}	82.92996
Europe	0.45	4.01×10^{-37}	222.3321
Africa	0.53	6.72×10^{-61}	406.0475
Asia	0.42	5.86×10^{-98}	586.9931
Australia	0.58	2.09×10^{-34}	238.1156
Atlantic Ocean	0.39	2.4×10^{-174}	1033.726
Indian Ocean	0.65	9.53×10^{-92}	726.9997
Pacific Ocean (West)	0.74	4.8×10^{-277}	2665.506
Pacific Ocean (East)	0.68	2.28×10^{-96}	807.7342

ACPD
14, 4303–4325, 2014

Table 2. Mean and standard deviation for aerosol hypothesis based and thermodynamic based annual flash rate.

Data source	OTD-LIS averaged annual flash rate ($fl\,yr^{-1}\,km^{-2}$)					Thermodynamic model averaged annual flash rate ($fl\,yr^{-1}\,km^{-2}$)					Averaged annual global flash rate from aerosol model ($fl\,yr^{-1}\,km^{-2}$)				
Regions	Land	Ocean	America (30° N –30° S)	Africa (30° N –30° S)	Maritime Continent (30° N–30° S)	Land	Ocean	America (30° N –30° S)	Africa (30° N –30° S)	Maritime Continent (30° N–30° S)	Land	Ocean	America (30° N –30° S)	Africa (30° N –30° S)	Maritime Continent (30° N–30° S)
Mean	6.5	0.5	16.0	12.4	11.2	5.5	0.7	18.9	5.2	13.0	5.9	0.65	11.5	8.5	9.7
Maximum	71.0	42.0	45.9	71.0	40.0	72.0	47.5	72.0	30.3	55.1	20.84	20.73	20.84	20.84	20.84
Minimum	0	0	0.3	0	0.45	0	0	0	0	0	0	0	1.1	0.77	0.8
Standard deviation	9.2	1.93	8.7	13.8	7.3	8.6	2.0	11.8	6.2	11.4	6.4	1.84	6.7	7.43	6.6

ACPD
14, 4303–4325, 2014

Table 3. Comparison in performance between two models, aerosol and thermodynamic hypothesis based.

Region	Model	RC	Lower 95 %RC	Upper 95 %RC	p value	F	Multiple R
Globe	Thermodynamic	0.73	0.71	0.74	0	7022.14	0.68
	Aerosol	1.	0.98	1.01	0	11 608.41	0.77
Land	Thermodynamic	0.66	0.62	0.7	4.5×10^{-211}	1237.463	0.62
	Aerosol	1.01	0.98	1.05	3.7×10^{-291}	1895.279	0.7
Ocean	Thermodynamic	0.4	0.38	0.43	3.8×10^{-254}	1275.046	0.4
	Aerosol	0.65	0.63	0.67	0	3572.599	0.6
North America	Thermodynamic	0.59	0.53	0.66	4.28×10^{-56}	335.5799	0.65
	Aerosol	0.88	0.81	0.97	1.75×10^{-63}	397.8354	0.69
South America	Thermodynamic	0.38	0.29	0.47	1.56×10^{-13}	62.90997	0.49
	Aerosol	0.79	0.63	0.95	4.57×10^{-19}	98.27883	0.58
Europe	Thermodynamic	0.41	0.31	0.50	3.22×10^{-13}	58.73972	0.42
	Aerosol	0.41	0.36	0.47	2.26×10^{-33}	192.0053	0.64
Africa	Thermodynamic	1.6	1.4	1.7	350.8713	350.8713	0.7
	Aerosol	1.3	1.21	1.48	5.91×10^{-60}	396.8437	0.73
Asia	Thermodynamic	0.44	0.4	0.48	3.51×10^{-96}	572.9739	0.64
	Aerosol	0.63	0.59	0.68	1.1×10^{-138}	950.4124	0.73
Australia	Thermodynamic	0.49	0.35	0.6	4.52×10^{-12}	55.30015	0.49
	Aerosol	1.3	1.14	1.44	4.27×10^{-38}	280.2102	0.79
Atlantic Ocean	Thermodynamic	0.31	0.29	0.38	2.88×10^{-36}	166.5138	0.31
	Aerosol	0.58	0.54	0.61	3.4×10^{-164}	957.1529	0.62
Indian Ocean	Thermodynamic	0.55	0.45	0.65	1.03×10^{-26}	121.5676	0.34
	Aerosol	0.94	0.89	1.0	2.1×10^{-161}	1096.113	0.73
Pacific Ocean (West)	Thermodynamic	0.29	0.27	0.32	8.96×10^{-5}	15.49943	0.57
	Aerosol	0.9	0.87	0.93	4.4×10^{-297}	3036.298	0.87
Pacific Ocean (East)	Thermodynamic	0.92	0.84	1.01	2.1×10^{-69}	470.7628	0.73
	Aerosol	0.93	0.87	0.99	7.4×10^{-113}	1068.565	0.86

ACPD
14, 4303–4325, 2014

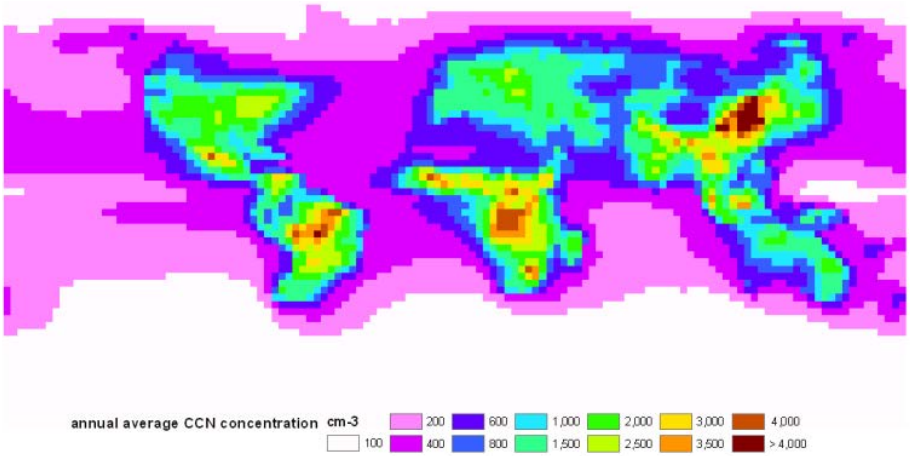

Fig. 1. Annual global cloud concentration nuclei concentration for 2008 (cm^{-3}).

ACPD
14, 4303–4325, 2014

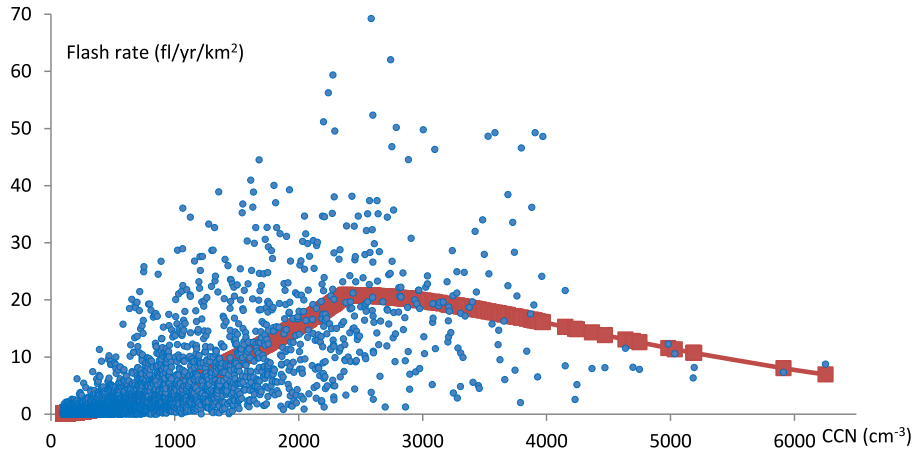

Fig. 2. Annually averaged flash rate by averaged, annual cloud condensation nuclei concentration. Blue dots – observation by OTD-LIS, red squares – model based on an aerosol hypothesis.

ACPD
14, 4303–4325, 2014

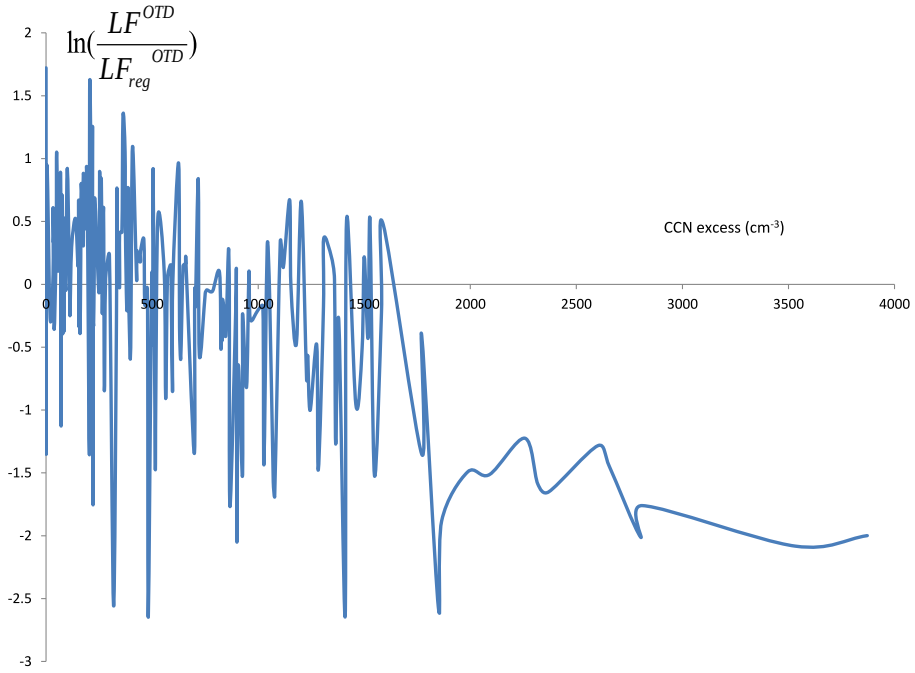

Fig. 3. Function of $\ln\left(\frac{LF^{OTD}}{LF_{reg}^{OTD}}\right)$ on the excess in CCN concentration N_{CCN}^{Excess} to critical value 2381 cm^{-3}.

ACPD
14, 4303–4325, 2014

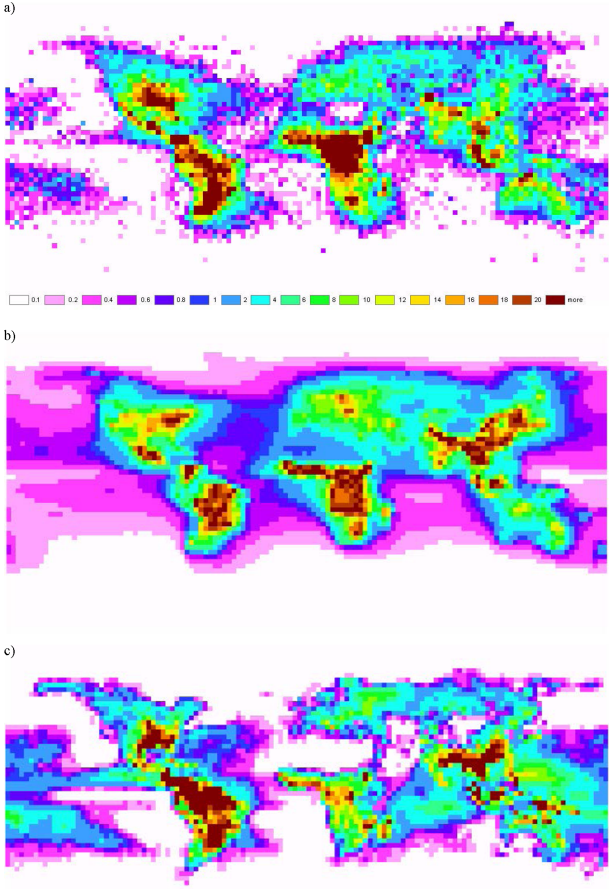

Fig. 4. The annual flash rate. **(a)** annually averaged for (1995–2000) OTD-LIS data, **(b)** model based on aerosol hypothesis, **(c)** model based on thermodynamic hypothesis.

ACPD
14, 4303–4325, 2014